Chinese Chemical Letters 37 (2026) 111760

Contents lists available at ScienceDirect

Chinese Chemical Letters

journal homepage: www.elsevier.com/locate/cclet

E. coli-mediated expedient biosynthesis of biotin-labeled ubiquitin probe enables activity-based profiling of deubiquitinases in cytoplasmic and nuclear compartments

Shuai Peng[a], Shaowen Wang[a], Xiaotong Liu[a], Hongrui Xu[b,*], Guoqiang Xu[a,c,d,e,*], Jia-Bin Li[a,*]

[a] *Jiangsu Key Laboratory of Drug Discovery and Translational Research for Brain Diseases, College of Pharmaceutical Sciences, The Fourth Affiliated Hospital of Soochow University, Jiangsu Province Engineering Research Center of Precision Diagnostics and Therapeutics Development, Jiangsu Key Laboratory of Preventive and Translational Medicine for Major Chronic Non-communicable Diseases, Suzhou Key Laboratory of Drug Research for Prevention and Treatment of Hyperlipidemic Diseases, Soochow University, Suzhou 215123, China*

[b] *Suzhou Municipal Center for Disease Control and Prevention, Suzhou 215004, China*

[c] *Suzhou International Joint Laboratory for Diagnosis and Treatment of Brain Diseases, College of Pharmaceutical Sciences, Soochow University, Suzhou 215123, China*

[d] *MOE Key Laboratory of Geriatric Diseases and Immunology, Suzhou Medical College of Soochow University, Suzhou 215123, China*

[e] *Suzhou Key Laboratory of Geriatric Neurological Disorders, the First People's Hospital of Taicang, Taicang Affiliated Hospital of Soochow University, Suzhou 215400, China*

ARTICLE INFO

Article history:
Received 6 June 2025
Revised 25 August 2025
Accepted 27 August 2025
Available online 28 August 2025

Keywords:
Activity-based ubiquitin probes
Chemical protein synthesis
Biotin-labeling
Deubiquitinase
Proteomic profiling

ABSTRACT

Deubiquitinases (DUBs) that remove conjugated ubiquitin from substrates are critical regulators of protein homeostasis and cellular signaling. Understanding the spatial distribution of DUBs in subcellular compartments is essential for uncovering their roles in stress responses and disease pathogenesis. Herein, we developed an *Escherichia coli* (*E. coli*)-based biosynthetic strategy for the expedient generation of biotin-labeled ubiquitin probe (Biotin-Ub-PA) through co-expression of Avi-Ub and BirA in *E. coli*, thus bypassing tedious chemical synthesis. Combined with affinity purification and proteomics, we utilized the biosynthetic probe to covalently capture active DUBs in subcellular compartments and revealed the distribution of DUBs in the cytoplasm and nucleus. As a proof of concept, hydrogen peroxide-induced activity changes of DUBs in the cytoplasm and nucleus were analyzed by the same probe. The results suggest that some DUBs, such as ubiquitin-specific protease 36 (USP36) and USP16, may undergo subcellular translocation and activity alterations under oxidative stress. Our study presents a reliable workflow for the spatial distribution analysis of DUBs under different stimuli or disease conditions.

© 2026 Published by Elsevier B.V. on behalf of Chinese Chemical Society and Institute of Materia Medica, Chinese Academy of Medical Sciences.

Ubiquitination, the covalent attachment of ubiquitin onto protein substrates, is a conserved and reversible post-translational modification (PTM) in eukaryotes, which governs virtually every cellular process through either proteolytic or non-proteolytic pathways [1,2]. Deubiquitinases (DUBs) that are responsible for the removal of ubiquitin from substrates are critical for the maintenance of ubiquitin homeostasis [3]. The regulatory expression and activity of DUBs serve crucial roles in many cellular activities, such as DNA damage repair [4,5], immune signaling [6–8], and chromatin remodeling [3,9]. Dysfunctions of DUBs are closely associated with the development of many diseases, including cancers [10–12], neurodegenerative [13,14] and autoimmune diseases [8], making DUBs attractive therapeutic targets. Thus, understanding the spatiotemporal activities and catalytic mechanisms of DUBs under physiological, pathological, and stress conditions, is not only critical for decoding the "ubiquitin code", but also facilitates the discovery of new therapeutic strategies.

Activity-based ubiquitin probes (Ub-ABPs) that mimic the substrates of DUBs and contain a reactive warhead to covalently crosslink with enzymes have emerged as powerful tools for the characterization of DUBs [15–19]. One of the most attractive ABPs is ubiquitin-propargylamide (Ub-PA) with different affinity tags, which exhibits high reactivity and selectivity towards the active cysteine in DUBs [20]. These Ub-PA probes have not only been applied in the activity-based enrichment of DUBs in biological samples for proteomic analysis, but also promote structure determi-

* Corresponding authors.
E-mail addresses: christinerania@163.com (H. Xu), gux2002@suda.edu.cn (G. Xu), lijiabin@suda.edu.cn (J.-B. Li).

https://doi.org/10.1016/j.cclet.2025.111760
1001-8417/© 2026 Published by Elsevier B.V. on behalf of Chinese Chemical Society and Institute of Materia Medica, Chinese Academy of Medical Sciences.

nation and inhibitor discovery of DUBs [21–30]. For instance, using the synthetic Halo/hemagglutinin (HA)-tagged Ub-PA, Kwasna *et al.* discovered ZUFSP as a novel DUB class that specifically cleaves K63-linked polyubiquitin chains [21]. Application of the synthetic biotin-labeled Ub-PA revealed that ubiquitin-specific protease 25 (USP25) was a highly expressed and active DUB in pancreatic ductal adenocarcinoma (PDAC) [23]. Ub-PA has also been used as a suicide substrate to covalently stabilize the catalytic complexes of DUBs (such as ovarian tumor protease (vOTU), ubiquitin carboxy-terminal hydrolase L5 (UCH-L5), and USP30), thereby facilitating their structure determination [20,24,25]. Furthermore, a 1:1 combination of Biotin-Ub-PA and Biotin-Ub-VME (vinyl methyl ester) was utilized to establish an activity-based protein profiling (ABPP) platform, which enabled the quick assessment of the activity and selectivity of chemical inhibitors against endogenous full-length DUBs [29].

Herein, we profiled the subcellular localization of DUBs and their distribution changes under cellular oxidative stress using biotin-labeled Ub-ABPs. To this end, we first developed an *Escherichia coli* (*E. coli*)-based biosynthetic strategy that integrates protein co-expression and ammonolysis reactions for the rapid preparation of probe Biotin-Ub-PA. Based on standard prokaryotic protein expression, the method allows the acquisition of Biotin-Ub-PA in large quantities. After activity validation of the probe, combined with subcellular fractionation, we characterized the localization of DUBs in HEK293T cells and explored the spatial distribution changes of DUBs in nucleoplasmic fractions under oxidative stress.

DUB-targeting ABPs usually contain a ubiquitin module, a reactive warhead, and a reporting module. For the enrichment of DUBs in complex samples, affinity tag-based reporting modules have become indispensable. Among them, HA and Flag tags have been extensively adopted owing to their ease of direct generation *via* expression. Compared to these two tags, the biotin tag exhibits superior performance in tolerating strong denaturing washing conditions to remove nonspecific binding proteins, which may maximize the advantage of ABP-based covalent enrichment. The current incorporation of a biotin-tag onto Ub-ABPs mainly relies on chemical synthesis [20,31,32] or *in vitro* enzymatic reaction (Figs. S1a and b in Supporting information) [33,34]. Although these methods exhibited high efficiency on the biotin labeling of ubiquitin, they are technically challenging or cumbersome for biochemical laboratories. Therefore, our study began with the preparation of biotin-labeled ubiquitin (Biotin-Ub).

Given that the biotin ligase BirA can specifically catalyze the installation of biotin onto a 15-amino acid peptide (Avi), thus enabling site-specific biotinylation of Avi-tagged proteins *in vitro* [33–35], we asked whether the Biotin-Ub can be directly produced in *E. coli* cells through the co-expression of Avi-tagged ubiquitin and BirA. The ubiquitin variant gene with an N-terminal Avi Tag and a Gly-to-Cys mutation at position 76 (Avi-UbG76C) was designed and cloned into vector pET-22b, and the BirA gene was cloned into vector pACYC-LIC. The two plasmids were then co-transformed into *E. coli* BL21 (DE3) cells (Fig. 1a, Figs. S1c and d in Supporting information). Considering that BirA was usually expressed at low temperatures of 16–18 °C while ubiquitin can be expressed in a wide temperature range of 16–37 °C, the initial co-expression of BirA and Avi-UbG76C was conducted at 16 °C, in the presence or absence of D-biotin. After 12 h, the cells were lysed and subjected to reversed-phase high-performance liquid chromatography (RP-HPLC) analysis. It showed that the addition of D-biotin resulted in complete disappearance of Avi-UbG76C, and generation of two new peaks. Of these, one (highlighted with a yellow background in Fig. 1b) matched the molecular weight of biotin-labeled Avi-UbG76C (Biotin-UbG76C), while the other (marked with "*" in Fig. 1b) exhibited a 131.5 Da higher molecular weight, which was consistent with the mass increase caused by the condensation of a

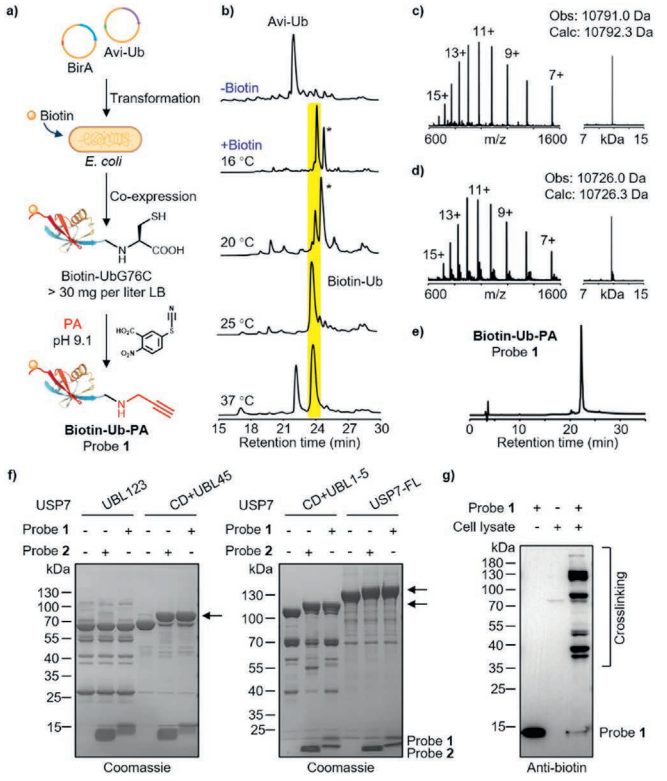


Fig. 1. Biosynthesis and characterization of the biotin-labeled ubiquitin probe. (a) Scheme of the *E. coli*-based biosynthesis of probe **1**, including the transformation of Avi-UbG76C and BirA genes into *E. coli* BL21 (DE3) cells, protein recombinant expression induced by isopropyl-β-D-thiogalactopyranoside (IPTG) in the presence of D-biotin, and activated cysteine-directed ammonolysis. (b) Analytical RP-HPLC traces (214 nm) of BirA-catalyzed biotinylation of Avi-UbG76C in *E. coli*. The peak in the yellow background indicates Biotin-UbG76C. * marked peak was speculated to be Biotin-Met-UbG76C. (c) ESI-MS analysis of Biotin-UbG76C. Deconvolutional mass spectra were generated by the UniDec software. (d, e) Analytical RP-HPLC and ESI-MS analyses of the purified probe **1**. (f) SDS-PAGE analysis of labeling of USP7 or its truncations by probe **1**. Arrows indicate crosslinked bands. (g) Western blot analysis of crosslinked proteins by probe **1** in HEK293T cells lysate.

methionine (Met) onto Biotin-UbG76C (Figs. 1b and c, Figs. S2a–c in Supporting information). Given that a Met was encoded as the starting amino acid in the Avi-UbG76C gene, the second peak was speculated to be N-terminal Met-retained Biotin-UbG76C (Biotin-Met-UbG76C, Fig. S2b).

To reduce incomplete excision of the starting Met, we increased the expression temperature, as higher temperatures may increase the expression or activity of methionine-specific aminopeptidase (MetAP), an enzyme responsible for the N-terminal Met cleavage in prokaryotic expression systems. The co-expression was further conducted at different temperatures of 20, 25 and 37 °C (Fig. S2a in Supporting information). Only trace amounts of Biotin-Met-UbG76C were generated at 25 and 37 °C, while expression at 20 °C resulted in higher proportion of Biotin-Met-UbG76C, as compared to expression at 16 °C (Fig. 1b). Although the expression level of ubiquitin mutant could be elevated at 37 °C, nearly half of the Avi-UbG76C was not labeled by biotin, probably due to the insufficient soluble expression of BirA at this temperature as compared to Avi-UbG76C (Fig. 1b and Fig. S2a in Supporting information). Hence, we conducted protein expression at 25 °C and then added 1 % (v/v) trifluoroacetic acid (TFA) to the ubiquitin- and BirA-co-expressed cell lysate to precipitate most impurities. Subsequent RP-HPLC purification generated >30 mg of Biotin-UbG76C from 1 L of LB culture medium, and the product was confirmed by electrospray ionization mass spectrometry (ESI-MS) (Fig. 1c). Note, the deconvolu-

tional MS and observed molecular weight were generated by the UniDec software [36].

We then utilized the activated cysteine-directed protein ligation (ACPL) method [37] to embed a propargylamine (PA) warhead into the C-terminus of ubiquitin to generate probe Biotin-Ub-PA (**1**) (Fig. S1d in Supporting information). The purified Biotin-UbG76C (0.2 mmol/L) was dissolved in an ammonolysis buffer (6.0 mol/L Gdn·HCl, 0.1 mol/L Na_2HPO_4, 1.0 mmol/L TCEP, pH 9.1), which was treated by 5.0 mmol/L 2-nitro-5-thiocyanobenzoic acid (NTCB) and 1.0 mol/L PA. After stirring at 37 °C for 12 h, the desired probe **1** was generated with an isolation yield of 48 %. Chromatographic and MS analyses confirmed the high purity and correct molecular weight of probe **1** (Figs. 1d and e). Further circular dichroism (CD) spectroscopy showed that the refolded **1** exhibited a characteristic absorption similar to that of recombinant ubiquitin, indicating that probe **1** has the correct secondary structure (Fig. S2d in the Supporting information). These results concluded that the combination of *in vivo* biotin-labeling on ubiquitin and ACPL-mediated *in situ* ammonolysis enabled the efficient preparation of biotin-labeled ubiquitin probes. This biosynthesis strategy avoids the repetitive purification of BirA and substrates for *in vitro* biotinylating reaction, as well as the laborious chemical synthesis, providing an expedient method to obtain biotin-labeled ubiquitin probes for biological laboratories.

Considering that probe **1** contains an additional Avi sequence (15 amino acids), we evaluated its crosslinking activity towards DUBs, as compared to the ubiquitin probe without any tag (Ub-PA, probe **2**). Probe **1** (10 μmol/L) was incubated with the known deubiquitinase USP7 or its truncations at 37 °C for 1 h, and probe **2** was used as a control (Figs. S2e and f in the Supporting information). Strong bands corresponding to the molecular weight of probe-enzyme adducts were detected, indicating that the newly synthesized probe **1** is capable of covalently capturing DUBs (Fig. 1f). Moreover, the crosslinking efficiency of probe **1** with USP7 or its active truncations (CD+UBL45 and CD+UBL1–5) was comparable to that of probe **2**, while the two probes could not react with the inactive truncation UBL123 (Fig. 1f). These results suggested that the introduction of Avi-tag at the N-terminus did not impair the reactivity of the probe towards DUBs. Subsequently, we used probe **1** to capture DUBs in the cell lysate. The probe **1** (2 μmol/L) was incubated with whole cell lysate at 37 °C for 1 h, followed by immunoblotting with an anti-biotin antibody. Multiple probe-crosslinked bands were observed and probe **1** was almost completely consumed, further confirming the high reactivity of probe **1** with DUBs in cell lysate (Fig. 1g and Fig. S2g in Supporting information). Moreover, cell lysates pretreated with the broad-spectrum DUB inhibitor PR-619 significantly weakened the intensities of the crosslinked bands of probe **1** with increasing inhibitor concentration (Fig. S2h in Supporting information). For example, in the case of USP7, the band intensities of USP7-probe **1** adduct were clearly weakened by PR-619 (Fig. S2h). These results demonstrated that probe **1** crosslinks DUB specifically and with high reactivity in cell lysates.

We next mapped the cellular localization of DUBs using probe **1**-mediated enrichment from different cell compartments (Fig. 2a). Cytoplasmic and nuclear fractions of HEK293T cells were prepared and immunoblotted with cytoplasmic and nuclear markers glyceraldehyde-3-phosphate dehydrogenase (GAPDH) and Lamin A/C, respectively (Fig. S3a in Supporting information). Subsequently, probe **1** was added to each of the two cell fractions and incubated by gently rotating at 37 °C for 1.5 h. The probe **1**-protein conjugates were enriched by the addition of streptavidin magnetic beads (Fig. 2a). Based on the strong affinity of biotin for streptavidin, we used multiple rounds of rigorous washing conditions (2 % SDS and 500 mmol/L NaCl) to remove non-covalently interacting proteins. The bound proteins were separated by sodium dodecyl

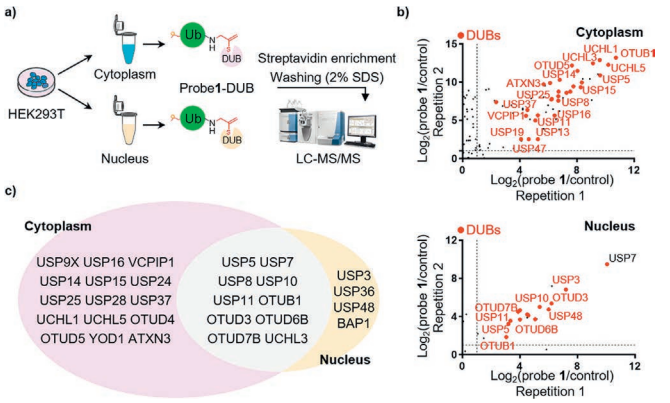


Fig. 2. Characterization of the distribution of DUBs in the cytoplasm and nucleus using probe **1**. (a) Schematic diagram of experimental process. (b) Scatter plots showing the DUBs enriched in cytoplasmic and nuclear fractions, respectively. Significantly enriched DUBs are denoted in red. (c) Venn diagram showing the overlap of captured DUBs in the nucleus and cytoplasm by probe **1**.

sulfate-polyacrylamide gel electrophoresis (SDS-PAGE) after elution by heating (98 °C for 10 min) and subsequently trypsinized for liquid chromatography-tandem mass spectrometry (LC-MS/MS) analysis. Enrichment experiments were conducted in two independent replicates, with streptavidin magnetic beads serving as a control. A total of 39 DUBs were detected in our experiment (Tables S1 and S2 in Supporting information), comparable to the previous studies [38]. Further scatter plot analysis showed that 25 DUBs were enriched in the cytoplasm and 14 DUBs were enriched in the nucleus (Fig. 2b). Among them, 10 DUBs were identified by enrichment in both cytoplasmic and nuclear components (Fig. 2c). In addition, we found that sentrin-specific protease 8 (SENP8) and several E3 ligases were also identified because of their weak crosslinking activity to Ub-ABP (Figs. S3b and c in Supporting information) [22,39]. The subcellular localization of the above-identified DUBs (16 USPs, 8 OTUs, 4 UCHs, and 1 Machado-Josephin domain-containing protease (MJD)) is consistent with the results from biological studies [9] and the description in the UniProt database. For example, USP9X, USP14, and UCHL1 are known to localize in the cytoplasm, while USP7, USP8, and OTUD3 are distributed in both the cytoplasm and nucleus. These results demonstrated the specificity and robustness of probe **1** in mapping the activity-based cellular localization of DUBs.

The spatial distribution of DUBs can remodel the interaction patterns of DUBs with other molecules and precisely regulate their intracellular activities and functions. Having confirmed the specificity and enrichment capacity of probe **1** through systematic validation (Figs. 1 and 2), we sought to investigate its application in mapping spatial dynamics of DUBs under stress conditions (Fig. 3a). As proof of concept, hydrogen peroxide (H_2O_2) was selected as a physiological stimulus to mimic oxidative stress that is a common challenge to cellular homeostasis and a major cause for DNA damage [10,40,41]. HEK293T cells were treated with 1.0 mmol/L H_2O_2 for 15 min to induce the stress [42]. After the subsequent removal of H_2O_2, cells continued to be cultured in a fresh medium. The generation of H_2O_2-induced oxidative stress was confirmed by detecting the changes of DNA damage marker γH2A.X. Compared to the cells without H_2O_2 treatment, the γH2A.X level significantly increased after 1 h, but returned to normal level after 4 h of continuous culture (Fig. 3b). According to previous studies [32], the cells were harvested at 4 h of recovery culture, and immediately subjected to subcellular fractionation for probe **1**-based DUB enrichment (Fig. 3c). The enrichment was performed using the strep-

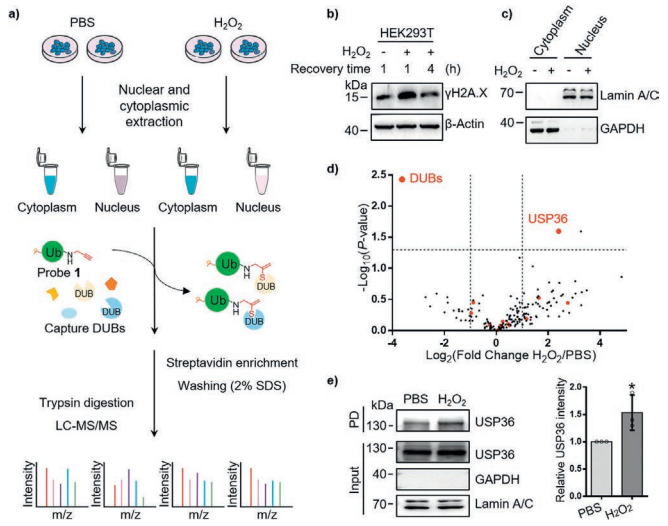


Fig. 3. Proteomic analysis of DUBs in nuclear and cytoplasmic components under H_2O_2-induced oxidative stress. (a) Schematic diagram of experimental process. (b) Immunoblotting to detect changes in γH2A.X after H_2O_2-treatment and recovery. (c) Evaluation of subcellular fractionation by immunoblotting. (d) The volcano plot for the enrichment of proteins in the cell nucleus by probe **1** after H_2O_2 or PBS treatment. DUBs are marked in red. (e) Pulldown experiment demonstrated an increase in USP36 enriched by probe **1** after H_2O_2 treatment ($n = 3$). Data are presented as mean ± standard deviation (SD). Student's *t*-test. $^*P < 0.05$.

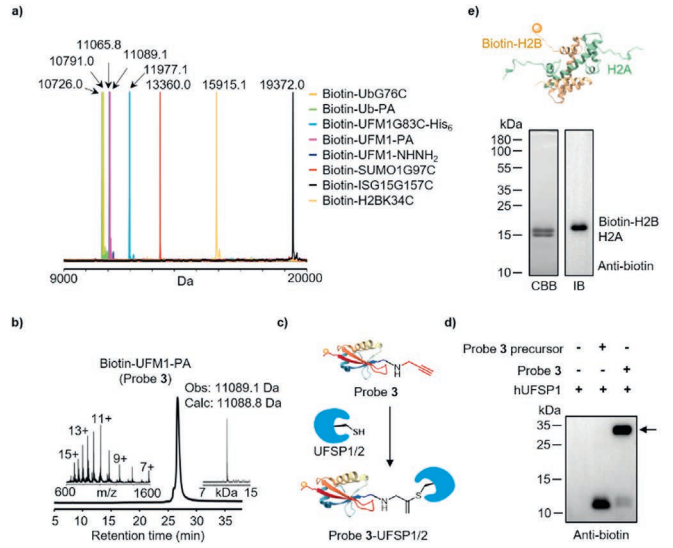


Fig. 4. *E. coli*-based biosynthesis of biotin-labeled ubiquitin-like proteins (UBLs), H2BK34C, and histone H2A-H2B heterodimer. (a) Integration of deconvolution MS of biotin-tagged Ub, UBLs (UFM1, ISG15, SUMO1), H2BK34C, and their derived probes. (b) Analytical RP-HPLC and MS analyses of the purified probe **3**. (c) Schematic diagram of the principle of probe **3** crosslinking UFSP1/2. (d) Western blot analysis of labeling of purified hUFSP1 by probe **3**. The arrow indicates a crosslinked band. (e) SDS-PAGE and Western blot analysis of purified biotin-tagged H2A-H2B heterodimer. The biotin tag is labeled at the N-terminus of H2B. CBB: Coomassie brilliant blue staining. IB: Immunoblotting.

tavidin magnetic beads described above. Three replicates of each pulldown experiment were performed, with PBS as the control.

The relative abundance of proteins in control and experimental groups with statistical significance ($log_2FC > 1$ or < -1, and *P*-values < 0.05) were calculated to generate the volcano plot. In the cytoplasm, upon oxidative stress, the intensity of some probe-enriched DUBs (*e.g.*, UCH-L5, USP8) generally decreases (Fig. S4a in Supporting information), indicating the impact caused by oxidative stress on the activity of some DUBs. This result may be related to the protein degradation process, which helps cells cope with oxidative stress and maintain cellular homeostasis [40]. In the nucleus, we also found that H_2O_2 treatment caused significant changes of some DUBs. For example, USP16 was only captured in H_2O_2-treated nucleus (Fig. S4b in Supporting information). By contrast, it was detected in both the H_2O_2-treated and untreated cytoplasm. It implied that H_2O_2 may cause nucleoplasmic shuttling of this enzyme although the underlying mechanism is not clear. We then validated this observation using immunofluorescence. As shown in Figs. S4c–e (Supporting information), compared with the control group where USP16 was dispersed in the nucleus and cytoplasm, the fluorescence signal of USP16 significantly increased in the nucleus and decreased in the cytoplasm after H_2O_2 treatment. Actually, USP16 is a known deubiquitinase that specifically removes ubiquitin from histone H2AK119 site [43], which is closely associated with DNA damage repair and gene transcription silencing.

Among the probe-captured DUBs, USP36 exhibited the largest increase in abundance after oxidative stress with a fold change (log_2FC) of 2.4 (Fig. 3d). Previous studies have demonstrated that USP36 can increase the stability of c-Myc and SOD2 through deubiquitination, and then regulate oxidative stress and renal cell protection [44]. In addition, it has been noted that in the presence of DNA replication stress, USP36 can increase the stability of PrimPol, thus helping cells to effectively respond to replication stress and maintain genome stability [45]. Our result that more USP36 was enriched after H_2O_2 treatment was consistent with the previous studies. For further validation, we conducted a pulldown experiment, which confirmed the increase of USP36 level in the nucleus under oxidative stress (Fig. 3e). These results suggested that the biotin-labeled Ub-ABP can efficiently analyze the subcellular activity changes of DUBs caused by H_2O_2-induced oxidative stress.

Besides ubiquitin, ubiquitin-like proteins (UBLs) also covalently modify protein substrates in cells, which play essential roles in protein stability, gene regulation, and other processes [46–49]. Given that the understanding of UBL-related biological regulation also requires biotin-tagged UBL-ABPs, we further extended the *E. coli*-based biosynthesis strategy to prepare biotin-labeled UBLs. Similarly, the N-terminal Avi-tagged UFM1, SUMO1, and ISG15 mutants were co-expressed with BirA in *E. coli* BL21 (DE3), respectively. The results of RP-HPLC and ESI-MS analysis showed that all the UBLs could be almost completely biotinylated, and their efficiencies were equivalent to that of ubiquitin (Fig. 4a and Figs. S5a–c in Supporting information). Of these, Biotin-UFM1G83C produced by *E. coli* was transformed into probe Biotin-UFM1-PA (**3**, Fig. 4b) to crosslink UFM1-specific proteases UFSP1/2. Compared with the non-reactive precursor (Biotin-UFM1-$NHNH_2$), probe **3** crosslinked recombinant human UFSP1 (hUFSP1) and endogenous UFSPs in cell lysate with high efficiency, which is consistent with the previous results of a chemically synthesized UFM1-ABP (Figs. 4c and d, Figs. S5d and e in Supporting information) [50]. Moreover, this biosynthetic strategy can also efficiently generate biotinylated histones (*e.g.*, H2BK34C) (Fig. S5f in Supporting information). Notably, histones are usually expressed in inclusion bodies of *E. coli*, different from the soluble expressed ubiquitin and UBLs. Besides these single-subunit proteins, a biotin-labeled histone H2A-H2B heterodimer was further efficiently prepared, which was successfully incorporated into histone octamers and nucleosome core particles (NCPs) with H3, H4 and 147-base pair of 601 DNA (Fig. 4e, Figs. S5g and h in Supporting information). It indicated that our *E. coli*-mediated *in situ* biotinylation may be applicable to diverse protein substrates, including soluble, insoluble proteins and protein complexes. Combined with other modern protein chemical synthesis technologies [51–61], this method may facilitate the ac-

quisition of chemically customized protein probes. Given that the ubiquitin, UBLs and histones used as examples in our study are structurally simple small proteins that can be readily expressed in *E. coli*, the extension of this strategy to biotin labeling of more complex substrates, such as membrane proteins, high-molecular-weight proteins, necessitates further investigation. Additionally, the potential structural and functional perturbations on some proteins caused by the Avi tag should be rigorously evaluated in each context.

In summary, we presented a reliable workflow from probe preparation to cell component-specific DUB enrichment for the spatial distribution analysis of DUBs under stimulus conditions. Our *E. coli*-mediated biosynthetic strategy enables rapid, low-cost, and scalable preparation of biotin-labeled ubiquitin and UBL probes, which can be easily implemented in most biochemical laboratories. Using the newly synthesized ubiquitin probe, we revealed the subcellular localization of most known DUBs and profiled their spatial changes under oxidative stress. Compared to the DUB analytical approaches based on non-covalent interaction profiling or untargeted proteomics [62,63], ABPs enable high-throughput screening of DUBs through activity-based covalent enrichment. However, previous applications of ABPs mainly focused on the DUB activity changes in whole cells [22,23,27,28], while our study provides a workflow for analyzing the subcellular distribution of DUBs. Although as a proof-of-concept study, we only analyzed the DUB changes in the nucleus and cytoplasm, by integrating the organelle separation techniques, we anticipate that this workflow could be extended to explore DUB changes in organelles such as mitochondria and endoplasmic reticulum. Given that probes with different warheads have been demonstrated to exhibit different cross-linking activities with DUBs [16,17], a hybrid platform composed of probes containing various warheads (such as propargylamide, azapeptide esters, vinylmethyl esters and viny sulfones) can be further prepared using our *E. coli*-mediated biosynthetic strategy, which may facilitate the identification of low-abundance or low-affinity DUBs in future studies.

Declaration of competing interest

The authors declare that they have no known competing financial interests or personal relationships that could have appeared to influence the work reported in this paper.

CRediT authorship contribution statement

Shuai Peng: Writing – review & editing, Writing – original draft, Validation, Investigation, Data curation. **Shaowen Wang:** Validation, Data curation. **Xiaotong Liu:** Validation, Data curation. **Hongrui Xu:** Writing – review & editing, Validation, Resources. **Guoqiang Xu:** Writing – review & editing, Supervision, Resources, Funding acquisition. **Jia-Bin Li:** Writing – review & editing, Writing – original draft, Supervision, Project administration, Funding acquisition, Conceptualization.

Acknowledgments

This work was supported by the National Natural Science Foundation of China (Nos. 22177085, 22477092, and 32171437), Suzhou International Joint Laboratory for Diagnosis and Treatment of Brain Diseases, Interdisciplinary Basic Frontier Innovation Program of Suzhou Medical College of Soochow University (No. YXY2302015), and the Suzhou Key Laboratory of Geriatric Neurological Disorders (No. SZS2024001).

Supplementary materials

Supplementary material associated with this article can be found, in the online version, at doi:10.1016/j.cclet.2025.111760.

References

[1] D. Komander, M. Rape, Annu. Rev. Biochem. 81 (2012) 203–229.
[2] K.N. Swatek, D. Komander, Cell Res. 26 (2016) 399–422.
[3] T.E.T. Mevissen, D. Komander, Annu. Rev. Biochem. 86 (2017) 159–192.
[4] Y. Li, K. Luo, Y. Yin, et al., Nat. Commun. 8 (2017) 15752.
[5] C. Wu, Y. Chang, J. Chen, et al., Nucleic Acids Res. 49 (2021) 11224–11240.
[6] M. Zhang, M.X. Zhang, Q. Zhang, et al., Cell Res. 26 (2016) 1302–1319.
[7] T. Liuyu, K. Yu, L. Ye, et al., Cell Res. 29 (2019) 67–79.
[8] J. Ren, P. Yu, S. Liu, et al., Adv. Sci. 10 (2023) e2303807.
[9] M.J. Clague, S. Urbe, D. Komander, Nat. Rev. Mol. Cell Biol. 20 (2019) 338–352.
[10] D. Mennerich, K. Kubaichuk, T. Kietzmann, Trends Cancer 5 (2019) 632–653.
[11] G. Dewson, P.J.A. Eichhorn, D. Komander, Nat. Rev. Cancer 23 (2023) 842–862.
[12] F. Liu, J. Chen, K. Li, et al., Mol. Cancer 23 (2024) 148.
[13] B. Qin, X. Chen, F. Wang, Y. Wang, Cell Death Discov. 10 (2024) 475.
[14] H.A. Do, K.H. Baek, Ageing Res. Rev. 69 (2021) 101367.
[15] P. Gopinath, S. Ohayon, M. Nawatha, A. Brik, Chem. Soc. Rev. 45 (2016) 4171–4198.
[16] X. Sui, Y. Wang, Y.X. Du, et al., Chem. Sci. 11 (2020) 12633–12646.
[17] S. Chanda, S. Atla, X. Sheng, et al., J. Am. Chem. Soc. 147 (2025) 17817–17828.
[18] S.W. Dong, J.S. Zheng, Y.M. Li, et al., Sci. China Chem. 67 (2024) 1060–1096.
[19] J. Zhang, H. Peng, Z.A. Chen, et al., Chin. Chem. Lett. 35 (2024) 108560.
[20] R. Ekkebus, S.I. van Kasteren, Y. Kulathu, et al., J. Am. Chem. Soc. 135 (2013) 2867–2870.
[21] D. Kwasna, S.A. Abdul Rehman, J. Natarajan, et al., Mol. Cell 70 (2018) 150–164 e156.
[22] K. Wendrich, K. Gallant, S. Recknagel, et al., Nat. Chem. Biol. 21 (2025) 746–757.
[23] J.K. Nelson, M.Z. Thin, T. Evan, et al., Nat. Commun. 13 (2022) 2070.
[24] M. Gersch, C. Gladkova, A.F. Schubert, et al., Nat. Struct. Mol. Biol. 24 (2017) 920–930.
[25] D.D. Sahtoe, W.J. van Dijk, F. El Oualid, et al., Mol. Cell. 57 (2015) 887–900.
[26] X.D. Tan, J.S. Bai, S. Ding, et al., Chin. Chem. Lett. 30 (2019) 743–746.
[27] W. Gui, C.A. Ott, K. Yang, et al., J. Am. Chem. Soc. 140 (2018) 12424–12433.
[28] A. Saha, R. Mousa, Y. Alalouf, et al., Angew. Chem. Int. Ed. 63 (2024) e202410135.
[29] W.C. Chan, X. Liu, R.S. Magin, et al., Nat. Commun. 14 (2023) 686.
[30] G. Gavory, C.R. O'Dowd, M.D. Helm, et al., Nat. Chem. Biol. 14 (2018) 118–125.
[31] D.S. Hameed, A. Sapmaz, L. Burggraaff, et al., Angew. Chem. Int. Ed. 58 (2019) 14477–14482.
[32] Y. Wang, J. Chen, X. Hua, et al., Angew. Chem. Int. Ed. 61 (2022) e202203792.
[33] Q. Zheng, T. Wang, G.C. Chu, et al., Angew. Chem. Int. Ed. 59 (2020) 13496–13501.
[34] Y. Wang, Q. Xia, X. Hua, et al., Chin. Chem. Lett. 34 (2023) 108010.
[35] M. Fairhead, M. Howarth, Methods Mol. Biol. 1266 (2015) 171–184.
[36] M.T. Marty, A.J. Baldwin, E.G. Marklund, et al., Anal. Chem. 87 (2015) 4370–4376.
[37] Y. Qiao, G. Yu, K.C. Kratch, et al., J. Am. Chem. Soc. 142 (2020) 7047–7054.
[38] P. Paudel, C.M. Banos, Y. Liu, Z. Zhuang, ACS Chem. Biol. 18 (2023) 837–847.
[39] T. Gan-Erdene, K. Nagamalleswari, L. Yin, et al., J. Biol. Chem. 278 (2003) 28892–28900.
[40] N.A. Snyder, G.M. Silva, J. Biol. Chem. 297 (2021) 101077.
[41] A. Tyagi, S. Haq, S. Ramakrishna, Redox Biol. 48 (2021) 102194.
[42] G.M. Silva, D. Finley, C. Vogel, Nat. Struct. Mol. Biol. 22 (2015) 116–123.
[43] H. Ai, Z. He, Z. Deng, et al., Nat. Struct. Mol. Biol. 31 (2024) 1745–1755.
[44] Q. Liu, W. Sheng, Y. Ma, et al., Biochem. Biophys. Res. Commun. 513 (2019) 502–508.
[45] Y. Yan, Z. Xu, J. Huang, et al., Nucl. Acid. Res. 48 (2020) 12711–12726.
[46] L. Cappadocia, C.D. Lima, Chem. Rev. 118 (2018) 889–918.
[47] T. Wang, J. Jiang, X. Zhang, et al., Trends Mol. Med. 30 (2024) 1061–1075.
[48] T. Wang, C. Li, M. Wang, et al., Angew. Chem. Int. Ed. 61 (2022) e202206205.
[49] C. Li, T. Wang, L. Liang, et al., Sci. China Chem. 66 (2023) 837–844.
[50] C. Chen, C. Lu, F. Li, et al., Chemistry 29 (2023) e202300414.
[51] H. Ai, Z. Tong, Z. Deng, et al., Chem 9 (2023) 1221–1240.
[52] M. Pan, Q. Zheng, S. Gao, et al., CCS Chem. 1 (2019) 476–489.
[53] L.J. Liang, G.C. Chu, Q. Qu, et al., Angew. Chem. Int. Ed. 60 (2021) 17171–17177.
[54] H. Ai, Z. Tong, Z. Deng, et al., Nat. Chem. Biol. 21 (2025) 668–680.
[55] Z. Tong, H. Ai, Z. Xu, et al., Nat. Struct. Mol. Biol. 31 (2024) 300–310.
[56] D. Han, Y. Cui, X. Deng, et al., J. Am. Chem. Soc. 147 (2025) 4135–4146.
[57] D. Han, X. Deng, Y. Cui, et al., Angew. Chem. Int. Ed. (2025) e202502884.
[58] Z. Deng, H. Ai, M. Sun, et al., Mol. Cell 83 (2023) 3080–3094 e3014.
[59] K. Zou, Y. Xiao, J. Yang, M. Wu, Chin. Chem. Lett. 35 (2024) 109497.
[60] J. Li, J. Chen, Q.L. Hu, et al., Chin. Chem. Lett. 36 (2025) 110126.
[61] Y. Ma, Y. Wang, F. Wang, et al., Chin. Chem. Lett. 36 (2025) 110546.
[62] J.Y. Lee, M. Shoaib, J.W. Choi, et al., J. Pharm. Anal. 14 (2024) 427–430.
[63] F. Feng, W. Zhang, Y. Cao, et al., Chin. J. Nat. Med. 23 (2025) 1016–1024.